Published in final edited form as:

Cell Microbiol. 2015 February ; 17(2): 147–163. doi:10.1111/cmi.12362.

The p60 and NamA Autolysins from *Listeria monocytogenes* Contribute to Host Colonization and Induction of Protective Memory

Ceena Chandrabos[1,#], **Saïdi M'Homa Soudja**[1,#], **Brian Weinrick**[1,2], **Marilyn Gros**[1], **Aurel Frangaj**[1], **Massilva Rahmoun**[3], **William R. Jacobs Jr.**[1,2], and **Grégoire Lauvau**[1,*]

[1]Albert Einstein College of Medicine, Department of Microbiology and Immunology, Bronx, NY, USA, 10461

[2]Howard Hughes Medical Institute

[3]Institut National de la Santé et de la Recherche Médicale U924, Groupe *Avenir*, Institut de Pharmacologie Moléculaire et Cellulaire, 06560 Valbonne, France

Abstract

Inducing long-term protective memory $CD8^+$ T cells is a desirable goal for vaccines against intracellular pathogens. However, the mechanisms of differentiation of $CD8^+$ T cells into long-lived memory cells capable of mediating protection of immunized hosts remain incompletely understood. We have developed an experimental system using mice immunized with WT or mutants of the intracellular bacterium *Listeria monocytogenes (Lm)* that either do or do not develop protective memory $CD8^+$ T cells. We previously reported that mice immunized with *Lm* lacking functional SecA2, an auxiliary secretion system of gram-positive bacteria, did not differentiate functional memory $CD8^+$ T cells that protected against a challenge infection with WT *Lm*. Herein we hypothesized that the p60 and NamA autolysins of *Lm*, which are major substrates of the SecA2 pathway, account for this phenotype. We generated *Lm* genetically deficient for genes encoding for the p60 and NamA proteins, Δ*iap*Δ*murA Lm*, and further characterized this mutant. Δp60ΔNamA *Lm* exhibited a strong filamentous phenotype, inefficiently colonized host tissues, and grew mostly outside cells. When Δp60ΔNamA *Lm* was made single unit (SU), cell invasion was restored to WT levels during vaccination, yet induced memory T cells still did not protect immunized hosts against recall infection. Recruitment of blood phagocytes and antigen-presenting cell activation was close to that of mice immunized with ΔActA *Lm* which develop protective memory. However, key inflammatory factors involved in optimal T cell-programming such as IL-12 and type I IFN (IFN-I) were lacking, suggesting that cytokine signals may largely

[*]**Correspondence should be addressed to GL:** Albert Einstein College of Medicine, Department of Microbiology and Immunology, 1301 Morris Park Avenue, Bronx, NY, 10461, USA. Ph: +1 718 678 1188, Fax: +1 718 678 1085, gregoire.lauvau@einstein.yu.edu.
[#]Both authors equally contributed to this work.

Author Contributions

C.C. and S.M.S. designed the study, performed most experiments, analyzed the data and contributed to writing of the paper. B.W. ran and interpreted the Mass Spectrometry, and contributed to writing of the paper. M.G. performed some of the protection and T cell assays *in vivo*. A.F. made the autolysin expression constructs. W.R.J. contributed to critical reading of the paper. G.L. designed the study, contributed to experiments, analyzed the data and wrote the paper.

The authors declare that no conflict of interest exists.

account for the observed phenotype. Thus altogether, these results establish that p60 and NamA secreted by *Lm* promote primary host cell-invasion, the inflammatory response and the differentiation of functional memory $CD8^+$ T cells, by preventing *Lm* filamentation during growth and subsequent triggering of innate sensing mechanisms.

Introduction

The development of protective vaccines against intracellular pathogens such as the Human Immunodeficiency Virus (HIV) or *Mycobacterium tuberculosis*, two highly successful health-threatening human pathogens, still requires a more thorough understanding of the cues that regulate the differentiation of long-lived protective memory cells, and in particular that of memory $CD8^+$ T cells (Harty *et al.*, 2008, Sallusto *et al.*, 2010). While many studies are contributing to better defining the key host factors that orchestrate such processes, often through the use of antibody neutralizing molecules or knockout mouse models, the precise sets of events that lead to the development of potent protective pathogen-specific memory during natural infections are usually poorly understood. For instance, immunization of mice with the intracellular bacterium *Listeria monocytogenes (Lm)* or the lymphochoriomeningitis virus (LCMV Armstrong) are well-established models to study the differentiation of protective memory $CD8^+$ T cells; both vaccination induce life-long host immunity against a challenge infection with otherwise lethal doses of these pathogens, yet the underlying mechanisms are still under intense investigations (Pamer, 2004, Moseman *et al.*, 2013). During immunization, the expression of pathogen-derived molecules plays a critical role to promote pathogen virulence and pathogenesis but also to drive optimal host immune responses. Thus, precisely defining the microbial factors that modulate the initial host immune response, and how, is key to further dissect these complex processes and design innovative vaccination strategies (Iwasaki *et al.*, 2010).

Using *Lm* genetically deficient for the SecA2 ATPase (ΔSecA2), an auxiliary secretion system found in several pathogenic gram-positive bacteria (Lenz *et al.*, 2003), we have previously established that mice immunized with ΔSecA2 *Lm* were not protected against a challenge infection with WT *Lm* contrary to mice immunized with WT or ΔActA *Lm* (Muraille *et al.*, 2007). We have also found that *Lm*-specific memory $CD8^+$ T cells from mice immunized with ΔSecA2 but not ΔActA *Lm*, were unable to transfer protection to primary infected recipient mice (Muraille *et al.*, 2007).

The NamA and p60 autolysins from *Lm*, a N-acetylmuramidase and a glutamyl-mesodiaminopimelate endopeptidase, are major substrates of the SecA2 secretory pathway and are suggested to digest *Lm*-peptidoglycans (PGNs) during bacterial growth (Wuenscher *et al.*, 1993, Lenz *et al.*, 2003, Machata *et al.*, 2005). They play an essential role in enabling efficient *Lm* division and pathogenesis *in vivo*, and may account for the inability of ΔSecA2 *Lm* to induce potent immunological memory in immunized mice (Muraille *et al.*, 2007, Narni-Mancinelli *et al.*, 2007). Herein, we hypothesized that p60 and NamA autolysins are key to program $CD8^+$ T cells to become fully functional memory cells. *Lm* lacking either or both of these autolysins were shown to form bacterial filaments and to inefficiently colonize the host (Machata *et al.*, 2005). p60 and NamA may impact T cell-priming by preventing *Lm*

filamentous phenotype and ease *Lm* access to antigen-presenting cells (APCs) and/or by releasing PGN products that are known to modulate cytosolic Pattern Recognition Receptor (PRR) triggering and subsequent host APC activation. To investigate these hypotheses, we have generated *Lm* bearing targeted deletions in genes encoding both the p60 and NamA proteins, Δp60ΔNamA *Lm*, and further characterized this mutant and its ability to induce an immune response in immunized mice. We found that Δp60ΔNamA *Lm* were mostly inefficient to invade primary host cells in the spleen of infected mice, likely because of strong filamentation. Subsequently, we show that Δp60ΔNamA *Lm* failed to induce memory $CD8^+$ T cells that could protect immunized hosts against a challenge infection with WT *Lm*. Interestingly, rescuing WT single unit (SU) phenotype of Δp60ΔNamA *Lm* at the time of immunization, restored initial cell invasion and APC activation close to non-filamentous ΔActA *Lm*, yet failed to restore robust inflammation and long-term protective memory. Thus collectively our results suggest that the p60 and NamA autolysins from *Lm* control the differentiation of protective memory $CD8^+$ T cells by (i) allowing the access of *Lm* to host cell cytoplasm and (ii) by promoting efficient cytosolic growth together with the release of immunogenic products essential to promote optimal inflammation such as cyclic di-nucleotides, PGN and others, at the time of T cell priming.

Results

Expression of the p60 and NamA autolysins by *Lm* during immunization is essential for immunological protection against recall infection with WT *Lm*

To investigate whether the p60 and NamA autolysins from *Lm* may account for the inability of ΔSecA2 *Lm* to induce memory $CD8^+$ T cells that protected immunized mice against challenge infection with WT *Lm* (Muraille *et al.*, 2007), we generated a knockout mutant of *Lm* lacking both autolysins. Briefly, ΔNamA *Lm* bearing a targeted deletion of the gene encoding for the NamA protein (Lenz *et al.*, 2003) were transformed with the pKSV7 transfer vector bearing a p60-targeting knockout construct and ΔNamA *Lm* knocked-out for the gene encoding the p60 autolysin on its chromosome were selected as previously described (Shen *et al.*, 1995). Deletion was confirmed by PCR using primers outside the knockout portion of the p60 DNA and further sequencing (**not shown**). We next investigated whether Δp60ΔNamA *Lm* induced protective immunological memory in mice. For this, we inoculated WT BALB/c mice with two distinct immunizing doses of Δp60ΔNamA *Lm*, or as controls PBS, WT, ΔSecA2 and ΔLLO *Lm* (Figure 1). Five weeks later, mice were challenged with 3×10^5 WT *Lm* and spleen and liver plated after 48 hrs. As anticipated, while mice immunized with WT *Lm* averaged ~5.5×10^3 and 8.4×10^5 viable bacteria in spleen and liver respectively, Δp60ΔNamA *Lm* exhibited ~2.2–17 and 10–110 million *Lm* CFUs, a 3–4 logs higher load of viable bacteria. The numbers of *Lm* CFUs in mice immunized with Δp60ΔNamA *Lm* were comparable to that of ΔSecA2 and ΔLLO *Lm*-immunized groups. Similar results were also obtained when mice were challenged with lower numbers (6×10^4) of WT *Lm* (Figure S1), and in WT C57BL/6 mice (**not shown**). Thus mice immunized with Δp60ΔNamA *Lm* did not control the challenge infection with WT *Lm*, establishing that p60 and NamA play an essential role in the development of long-term protective memory.

Lack of p60 and NamA autolysins induces filamentation of *Listeria monocytogenes*

We next characterized the phenotype of mutants lacking both p60 and NamA autolysins compared to WT and ΔSecA2 *Lm* (Figure 2). While WT *Lm* formed smooth round-shaped colonies, ΔSecA2 and Δp60ΔNamA *Lm* exhibited rough, irregular shaped colonies (Figure 2A). Gram staining and microscopic analysis of Δp60ΔNamA *Lm* revealed that they formed long filamentous chains of bacteria with an average length of several tens of microns, in stark contrast with WT *Lm* that represented single units of 1–2 microns. These results, consistent with previous studies that had generated a similar mutant of *Lm* autolysins (Wuenscher *et al.*, 1993, Machata *et al.*, 2005), established that knocking-out the expression of both p60 and NamA autolysins in *Lm* induced drastic changes in *Lm* morphology and a bacterial chaining filamentous phenotype.

Δp60ΔNamA *Lm* inefficiently invade cells and colonize mouse tissues

Since Δp60ΔNamA *Lm* exhibited such a marked filamentous phenotype, we reasoned that they would likely be impaired in their ability to invade cells and tissues, and therefore have lower virulence. To assess this hypothesis, we inoculated WT mice intravenously (i.v.) with 0.6×10^7 Δp60ΔNamA *Lm*, a dose that corresponds to ~$0.1\times LD_{50}$ (**not shown**), and with 0.6×10^5 ΔSecA2 and 10^6 ΔActA *Lm* (Figure 2B), and monitored splenic bacterial growth over a 72 hour time course. ΔActA *Lm* lacks ActA, an important virulence factor of *Lm* required for cellular actin polymerization, which confers *Lm* intracytosolic motility and cell-to-cell spreading. ΔActA *Lm* exhibits impaired virulence similarly to ΔSecA2 *Lm*, yet does not form any bacterial chains. While all mutants exhibited comparable growth kinetics, filamentous *Lm* -ΔSecA2 and Δp60ΔNamA *Lm*- poorly colonized the spleens early on (2 hrs) compared to non-filamentous ΔActA *Lm*, and were cleared significantly faster with at least 2 logs less viable bacteria over the first 48 hrs post-inoculation. Together, these results suggested that the low virulence of Δp60ΔNamA *Lm* is accounted for by inefficient initial invasion of target cells within the spleen and faster clearance.

Filamentation promotes *Lm* extracellular growth inside infected tissues and survival in blood

While filamentous *Lm* did not efficiently invade the spleen, they still multiplied by a factor of ~50 over 24 hrs (Figure 2B). We hypothesized that growth of Δp60ΔNamA *Lm* mostly occurred outside cells yet inside infected spleens. To test this possibility, we injected mice with ΔActA or Δp60ΔNamA *Lm*, treated them or not with gentamycin 1 hr later to kill extracellular *Lm*, and plated spleens after 2 and 12 hrs to enumerate viable bacteria (Figure 2C). As expected, most ΔActA *Lm* were intracellular (>90%) whereas only ~40% (factor of 2.6) and 25% (factor of 4) of viable Δp60ΔNamA *Lm* were recovered from within cells at 2 and 12 hrs post-immunization, respectively. Moreover, the number of viable *Lm* CFUs increased in all groups between 2 and 12 hrs post immunization, with the highest in mice immunized with ΔActA *Lm* (factor of 23) most likely because ΔActA *Lm* had divided and formed independent CFUs inside infected cells. The number of Δp60ΔNamA *Lm* CFUs also increased (factor of 12), of which 50–75% was accounted for by extracellular growth. Of note, by 2 hrs post-immunization, the number of viable bacteria recovered from infected spleens was lower by a factor of ~35 in mice that received Δp60ΔNamA compared to ΔActA

Lm. Analysis of *Lm* viability in the blood early after injection, e.g., at 1, 5, 10, 30, 60 and 120 min (Figure 2D), suggested that filamentation increased the persistence of *Lm* in the blood, likely because of inefficient access to tissues, as observed in the spleen. Thus, collectively, filamentation substantially impairs the ability of *Lm* to access tissues and invade cells, and to establish a successful infection. Unexpectedly, filamentation promoted the unusual growth of *Lm* outside cells yet inside infected spleens.

Single unit Δp60ΔNamA *Lm* efficiently enter cells

Our results suggest that *Lm* chaining, which directly results from the lack of p60 and NamA autolysins, impairs the bacterium's ability to invade cells. Since cytosolic growth of *Lm* is a prerequisite to prime long-term *Lm*-specific protective memory (Berche *et al.*, 1987), it is likely that mice immunized with Δp60ΔNamA *Lm* cannot control recall infection simply because these mutants do not access host cells. Alternately, it is possible that the p60 and NamA autolysins are required independent of their effect on *Lm* filamentation, possibly through the release of PGN or other products with strong immunomodulatory activities. To explore these hypotheses, we set out to rescue the WT single unit (SU) phenotype in Δp60ΔNamA *Lm* using two different experimental approaches. First, we supplemented Δp60ΔNamA *Lm* during growth *in vitro* using a filtered culture supernatant of ΔLLO *Lm* grown to stationary phase (e.g., overnight, OVN), which contains the secreted p60 and NamA autolysins but not LLO (Lenz *et al.*, 2003) (Figure 3A, B). Bacteria were inoculated in a 1:1 or 1:0 ratio of OVN:fresh BHI media and grown either to log or stationary phases. While Δp60ΔNamA *Lm* grown in 100% fresh BHI medium formed long filaments (log-phase) and segregated in 'cotton-like' pellets, Δp60ΔNamA *Lm* grown in p60 and NamA-containing BHI grew as dense cultures (Figure 3A) and formed shorter filaments of intermediate length (1:1 ratio, Int-Δp60ΔNamA) to single unit (1:0 ratio, SU-Δp60ΔNamA) bacteria. As a second approach, recombinant p60 (rp60) and NamA (rNamA) were produced and purified from BL21 *Escherichia Coli* bacteria. Log-phase grown Δp60ΔNamA *Lm* incubated with purified autolysins became single bacterial units (Figure 3B). Quantification by microscopy analysis revealed that Δp60ΔNamA and ΔSecA2 *Lm* exhibited chains with an average of 70 and 16 single units *Lm* respectively. When cultured in presence of BHI-containing p60 and NamA autolysins, or digested with the purified hydrolases, the length of Δp60ΔNamA *Lm* was 16 (1:1) or 2 (1:0 and also with purified rp60 and rNamA), with the latter conditions being comparable to ΔActA *Lm*. These results were also confirmed using cytofluorometry and GFP-expressing *Lm* to determine the relative sizes (FSC) of the various bacterial suspensions, which varied by at least a factor of 50 (Figure S2A).

Taking advantage of SU-Δp60ΔNamA *Lm* obtained upon digestion with purified autolysins, we first tested whether invasion of macrophages could be restored *in vitro*. We infected WT bone marrow-derived macrophages (BMMP) with SU-Δp60ΔNamA, Δp60ΔNamA, or ΔActA *Lm*, and measured viable bacterial numbers recovered from these cells 2 hrs later (Figure S2B). Comparable numbers of viable bacterial CFUs (~10^4) were recovered from 2 hrs-infected macrophages in both conditions, suggesting that shortening to SU-Δp60ΔNamA *Lm* restored the ability of Δp60ΔNamA *Lm* to invade BMMP *in vitro* similarly to ΔActA *Lm*. Using GFP^+ *Lm*, we further confirmed that reducing the length of Δp60ΔNamA *Lm* (Int to SU) proportionally improved their ability to invade host cells *in vivo*, achieving

comparable frequencies of GFP^+ cells between SU-Δp60ΔNamA, ΔActA and ΔLLO *Lm* 1 hr post infection (Figure 3C). This was also observed by enumerating *Lm* CFUs recovered from the spleens of mice 2 hrs post infection wherein SU-Δp60ΔNamA or ΔActA formed equivalent numbers of viable *Lm* CFUs (~10–12,000), while only ~2,000 *Lm* CFUs were recovered from mice immunized with Δp60ΔNamA *Lm* (Figure 3D, **upper graph**). To provide formal demonstration that SU-Δp60ΔNamA *Lm* invaded host cells, we inoculated bacterial suspensions as before and one hour later treated mice (or not) with gentamicin for another hour before enumerating *Lm* splenic CFUs to discriminate between intracellular and extracellular bacteria (Figure 3D). SU-Δp60ΔNamA *Lm* entered cells as efficiently as ΔActA *Lm* with ~16,000 CFUs recovered from gentamicin-treated infected spleens, in contrast to 'full-length' Δp60ΔNamA *Lm* with only ~700 CFUs. This further established that filamentation dramatically reduces bacterial ability to enter spleen cells. Of note, between 2 and 12 hrs, SU or full-length -Δp60ΔNamA *Lm* grew similarly both outside or inside spleen cells. As expected, gentamycin injection mostly decreased *Lm* loads in mice that receive the filamentous mutant with ~40 (2 hrs) and 80 % (12 hrs) of viable Δp60ΔNamA *Lm* that were sensitive to gentamicin, correlating with extracellular growth in the host (Figure 3D, **lower panel**). In summary, our data implicate p60 and NamA autolysins as key regulators of *Lm* invasion of host tissues and cells, by allowing *Lm* separation to SU bacteria during growth. Altogether, these results support the idea that the low virulence associated with filamentous *Lm* may be fully accounted for by such 'physical impairment'.

Rescuing Δp60ΔNamA *Lm* entry to cells does not restore protective memory in immunized mice

Our results show that the lack of p60 and NamA autolysins acts as a "mechanical brake" to efficient colonization of the host by *Lm*, subsequently accounting for inadequate T cell priming and the inability of mice immunized with Δp60ΔNamA *Lm* to resist recall infection with WT *Lm* (Figure 1). If allowed to access host tissues and cells as SU bacteria, we reasoned that Δp60ΔNamA *Lm* could indeed prime long-term protective immunity in immunized hosts. Since SU-Δp60ΔNamA *Lm* could invade host cells as efficiently as ΔActA *Lm in vitro* and *in vivo*, we next tested whether WT BALB/c mice immunized with SU Δp60ΔNamA or Δp60ΔNamA and WT *Lm* as control groups were protected against challenge infection with WT *Lm* (Figure 4). Data show that mice vaccinated with SU-Δp60ΔNamA *Lm* exhibited ~100-fold more viable bacteria in their organs -spleen and liver- compared to protected hosts, thus did not control the challenge infection. Therefore, despite efficient entry into host cells, SU-Δp60ΔNamA *Lm* could not prime long-term protective memory, possibly as a result of poor growth *in vivo* and/or failure to promote adequate T cell priming environment.

Immunization with single-unit Δp60ΔNamA *Lm* restores robust recruitment of blood-derived $Ly6C^+$ monocytes and neutrophils

To gain further insights into why mice immunized with SU Δp60ΔNamA *Lm* were not protected against virulent challenge infection, we next conducted a systematic investigation of the T cell priming environment at the time of vaccination. Optimal T cell priming correlates with strong recruitment and activation of sentinel cells from the innate immune

system (Iwasaki *et al.*, 2004, Reis e Sousa, 2006). In mice immunized with ΔActA *Lm*, which develop strong protective $CD8^+$ T cell memory, blood phagocytes -e.g., $Ly6C^+$ inflammatory monocytes ($CD11b^{hi}Ly6C^{hi}$) and neutrophils ($CD11b^{hi}Ly6C^{dim}$)- are massively recruited to infected spleens, with peak recruitments between 24–48 hrs after the immunization (Figure 5A). In contrast, in mice that received Δp60ΔNamA *Lm* or ΔLLO *Lm* as control, only weak recruitment of these cells was observed, correlating with inefficient priming of long-term immunity. Thus, we next tested whether shortening Δp60ΔNamA *Lm* still promoted more efficient recruitment of these phagocytes to infected spleens (Figure 5B). We found that Int- and SU- Δp60ΔNamA *Lm* proportionally increased the frequencies of $Ly6C^+$ monocytes and neutrophils recruited to infected spleens, with frequencies becoming closer to that induced upon ΔActA *Lm* immunization. In line with these results, CCL2 and CXCL1, two major chemokines respectively regulating $Ly6C^+$ monocytes and neutrophil mobilization during inflammation increased by a factor of ~30–40 (SU-Δp60ΔNamA and ΔActA) compared to mice immunized with full length Δp60ΔNamA or ΔLLO *Lm*. Thus, *in vitro* rescue of filamentous Δp60ΔNamA to SU *Lm* restored their tissue and cell invasiveness *in vivo*, which subsequently promoted robust recruitment of blood-derived phagocytic effector cells, suggesting that this unlikely accounts for the impaired priming of T cells.

Antigen-presenting cell activation, but not overall inflammation, is largely restored by immunization with single-unit Δp60ΔNamA *Lm*

Strong activation of APCs is key to optimal T cell priming and differentiation into functional memory cells (Muraille *et al.*, 2005, Reis e Sousa, 2006). In mice immunized with ΔActA *Lm*, splenic $CD8\alpha^+$ $CD11c^{hi}$ DCs -the major APC subset involved in $CD8^+$ T cell priming (Heath *et al.*, 2004, Hildner *et al.*, 2008)- and $Ly6C^+$ monocytes underwent strong activation peaking between 24–48 hrs post-immunization, as measured by cell-surface upregulation of MHC class II and costimulatory molecules (CD80, CD86, CD40), and Sca-1 and IL-15 receptor alpha (IL-15Rα) two interferon-responsive cell-surface markers (Figure 6B, S2 **and not shown**) (Beuneu *et al.*, 2011, Soudja *et al.*, 2012). In contrast, only weak activation was found in groups that received Δp60ΔNamA or ΔLLO *Lm* (Figure 6C). As observed for blood phagocyte recruitments, shortening Δp60ΔNamA *Lm* proportionally restored strong maturation of APCs with upregulation of MHC-II, costimulatory molecules, the IFN responsive markers Sca-1 and IL-15Rα to levels close to those observed upon ΔActA *Lm* immunization (~70% of maximum upregulation).

However, while increased compared to full length Δp60ΔNamA *Lm*, peak levels (24 hrs (Campisi *et al.*, 2011)) of the splenic proinflammatory cytokines TNF-α, IL-12, IFN-γ, IFN-α, but not IL-10, were only partially restored in mice immunized with SU Δp60ΔNamA *Lm*, with levels only reaching up to 20–45% of those measured in mice immunized with ΔActA *Lm* (Figure 6D). Therefore, when enabled to access host cell cytoplasm, Δp60ΔNamA *Lm* could rescue the activation of APCs to substantial extends, yet not inflammatory cytokine levels. Thus while antigen and costimulatory signals were close to those found in mice immunized with ΔActA *Lm*, inflammatory cytokines remained largely impaired, which may account for the defective T cell priming and differentiation.

Levels of secreted cyclic-di-AMP, a potent bacterial inducer of type I IFN, are comparable between WT and mutant *Lm*

Amongst the inflammatory molecules with impaired secretion in mice immunized with SU Δp60ΔNamA *Lm*, type I IFN is an important modulator of T cell differentiation (Tough, 2012). Since recent reports provided strong evidence that cyclic diadenosine monophosphate (c-di-AMP) secreted by *Lm* is a major trigger of the IFN-I pathway (Woodward *et al.*, 2010), we hypothesized that Δp60ΔNamA *Lm* may secrete a lower amount of this compound. To test this possibility, we analyzed log-phase grown *Lm* supernatants for the presence of c-di-AMP using ultra-performance liquid chromatography-coupled mass-spectrometry (UPLC-MS). Because the amount of c-di-AMP (659.11 m/z) detected in culture supernatants was very low, we decided to monitor the 330.06 m/z fragment ion, which we could detect at higher levels as seen on representative MS chromatograms (Figure 7A). This ion, a product of in-source fragmentation exhibits the same retention time as intact c-di-AMP but is detected with a ~60% greater intensity, both in a commercial c-di-AMP sample (Invivogen, upper panel) and in a culture supernatant from WT *Lm* (lower panel). Of note, the quantity detected in the supernatants only represented ~2.5% of the signal detected in the standard (~1.5μg). Using this approach, we compared supernatants from log-phase grown SU-Δp60ΔNamA, Δp60ΔNamA, ΔActA and WT *Lm* (Figure 7B). As shown from the average of 4 independent replicate quantification experiments, sample variability was high and no significant differences in c-di-AMP abundance could be measured in the culture supernatants from the distinct bacteria. As an additional control, we used supernatants from WT L028 *Lm* that was reported to over secrete c-di-AMP (Schwartz *et al.*, 2012), and indeed detected substantially greater levels of c-di-AMP secreted by this WT *Lm* strain compared to WT 10403s (factor >10, **not shown**). Consistent with this result, infection of bone-marrow macrophages (BMMP) with SU-Δp60ΔNamA, but not ΔLLO or Δp60ΔNamA *Lm*, induced both IFNα and IFNβ genes to comparable extent as ΔActA or WT *Lm* (Figure 7C). Thus these results suggest that intrinsic differences in c-di-AMP secretion are unlikely to account for the lower levels of type I IFN measured in the spleen of mice immunized with SU-Δp60ΔNamA *Lm*, and that the early wave of type I IFN -and possibly other inflammatory cytokines- is equivalent in WT and mutant *Lm*. Therefore, the lack of overall inflammation in mice vaccinated by SU-Δp60ΔNamA compared to ΔActA *Lm* is most likely accounted for by inefficient growth of the filamentous mutant *in vivo*.

p60 and NamA autolysins contribute to key inflammatory signals required for effective differentiation of protective memory CD8$^+$ T cells *in vivo*

SU-Δp60ΔNamA *Lm* accessed host cell cytoplasm with comparable efficiency as ΔActA *Lm*, and promoted robust activation of antigen-presenting cells, yet the inflammatory environment and protective memory development was impaired (Figure 4–Figure 6). While our data favor the idea that the major impact of the p60 and NamA hydrolases on inflammation is related to their direct effect on the ability of *Lm* to divide and colonize tissues *in vivo*, it is still possible that the release of PGN digestion fragments or other molecules from *Lm* by these hydrolases possess PRR-triggering proinflammatory activities. To achieve better understanding of how p60 and NamA autolysins alter CD8$^+$ T cell differentiation, we next monitored CD8$^+$ T cells recognizing the K^d-restricted, naturally

presented $LLO_{91–99}$ epitope from *Lm* by measuring $LLO_{91–99}/K^d$ (tet^+) $CD8^+$ T cell frequencies over time in the blood of WT BALB/c ($H\text{-}2^d$) mice immunized with WT, Δp60ΔNamA, SU-Δp60ΔNamA and ΔActA *Lm* (Figure 8A, B **and not shown**). We chose to monitor $LLO_{91–99}/K^d$ (tet^+) $CD8^+$ T cells as these cells were shown to be sufficient to confer protection to infected host (Harty *et al.*, 1992). While maximum peak frequencies of tet^+ cells in mice immunized with WT were measured 7 d post infection, mice that received full length and SU Δp60ΔNamA and ΔActA (**not shown**) *Lm* peaked ~2 d earlier, most likely as a result of massive initial antigen loads. In all groups, however, comparable numbers of LLO-specific $CD8^+$ T cells were measured when reaching the memory stage (d 35) (Figure 8C), suggesting that functional differences in LLO-specific memory $CD8^+$ T cells most likely accounted for the lack of effective immunity in mice immunized with SU-Δp60ΔNamA or Δp60ΔNamA *Lm* compared to those that received WT or ΔActA *Lm* (Figure 1). Further analysis of LLO-specific memory $CD8^+$ T cells in all groups of immunized mice showed that the proportion of memory $CD8^+$ T cells that expressed effector markers associated with host protection, e.g., CCL3/MIP1Δ, granzyme B (cytolysis) and KLRG1, were significantly diminished in mice that received Δp60ΔNamA, SU Δp60ΔNamA or control ΔSecA2 *Lm* but not WT or ΔActA *Lm* (Figure 8C). Consistent with our previous work analyzing mice immunized with ΔSecA2 *Lm* (Narni-Mancinelli *et al.*, 2007), the proportion of central versus effector memory ($CD62L^{hi/lo}$) and of IFN-Δ^+ memory $CD8^+$ T cells was comparable between all groups. We could also confirm these observations on the C57BL/6 genetic background, using a transgenic mouse line that expresses $H2\text{-}K^d$ on the WT B6 background (Serbina *et al.*, 2003). Altogether, these results supported the idea of an altered pattern of differentiation of *Lm*-specific memory $CD8^+$ T cells in non-protected immunized mice.

Results in figure 5C suggested that immunization with SU-Δp60ΔNamA *Lm* largely fails to rescue strong inflammatory signals at the time of T cell priming, which are known to play key roles in programming T cell differentiation (Haring *et al.*, 2006). As an attempt to rescue protective memory, we provided strong MyD88-dependent inflammatory signals by co-immunizing mice with CpG oligonucleotides and SU-Δp60ΔNamA *Lm*, challenged these mice five weeks later with WT *Lm* and determined *Lm* titers after 2 d (Figure 8D). Whether these mice received CpG or not, bacterial titers in the spleen and the liver were comparable with $2.5–6\times10^6$ *Lm* CFUs, i.e., ~1.5–2 logs more bacteria than in protected mice. Interestingly however, analysis of LLO-specific $CD8^+$ T cells in the blood 8 and 21 d post immunization and before challenging these mice, showed that co-immunization with CpG rescued the differentiation of effector-type $KLRG1^+$ $CD8^+$ T cells, similarly to mice immunized with WT or ΔActA *Lm* (Figure 8E). However, these cells were quickly lost from the blood of CpG co-immunized mice compared to non-CpG or WT and ΔActA *Lm*-immunized groups, possibly accounting for the observed lack of protection. In summary, our data suggest that *Lm* p60 and NamA autolysins promote optimal $CD8^+$ T cell priming by regulating a complex network of inflammatory signals inside infected host cell cytoplasm, resulting from inefficient tissue colonization by filamentous *Lm*.

Discussion

Our results provide novel evidence that the inability of ΔSecA2 *Lm* to induce protective memory $CD8^+$ T cells is accounted for by impaired secretion of the p60 and NamA autolysins, two major substrates of this auxiliary secretory pathway. We show that through the control of *Lm* separation during multiplication, p60 and NamA prevent *Lm* cording/ filamentous phenotype, subsequently promoting efficient invasion of host cells. We also show that p60 and NamA autolysins play a key role in triggering strong inflammation during cytosolic growth of *Lm*, amongst which type I IFN, IL-12, TNF-α and IFN-γ. Interestingly, once *Lm* escapes to the cytosol of host cells, whether *Lm* expressed the autolysins or not, upregulation of cell-surface costimulatory molecules on APCs and recruitment of blood phagocytes were only moderately affected. Altogether, our results suggest that by controlling two essential steps, e.g., cell invasion and cytosolic-driven inflammation, p60 and NamA autolysins act as essential regulators of $CD8^+$ T cell programming and differentiation.

Previous studies have established the requirement for p60 and NamA PGN hydrolases in allowing *Lm* separation during growth, therefore preventing its filamentation (Wuenscher *et al.*, 1993, Machata *et al.*, 2005). Other reports have also documented that reduced secretion of p60 and NamA accounted for the filamentous, rough colony phenotype of ΔSecA2 *Lm*, which affected its ability to colonize the host, even though only ~50% of p60 and NamA are secreted through this secretory pathway (Lenz *et al.*, 2002, Lenz *et al.*, 2003). Using ΔSecA2 *Lm*, we have found that immunized mice did not develop robust $CD8^+$ T cell memory, yet increasing the immunizing dose of ΔSecA2 *Lm* from 0.1 (usual) to $1\times LD_{50}$ restored protective T cell responses against challenge infection with WT *Lm* (Campisi *et al.*, 2011). This suggested that increasing the cytosolic concentration of these *Lm* proteins that are partially secreted independently of SecA2, could restore signals essential to program protective $CD8^+$ T cell memory. Following up on these early findings, current results show that without p60 and NamA, even with very high immunizing doses of SU Δp60ΔNamA *Lm*, mice remain unable to mount protective memory responses, consistent with the idea that p60 and NamA account for the inability of ΔSecA2 *Lm* to induce strong CD8 memory.

Our results highlight two distinct mechanisms by which p60 and NamA *Lm* autolysins affect T cell differentiation, that are both related to their essential role in allowing separation of *Lm* bacteria following division. Lack of these enzymes induces remarkable *Lm* cording with filaments of several tens of microns constituted of ~70–80 units of *Lm*. Such unusual length represent the first major mechanism that prevents *Lm* invasion of host cells as a result of a 'physical' impairment, e.g., inability to be efficiently phagocytosed by marginal zone / red pulp macrophages and to be targeted to DCs for efficient shuttling to spleens (Muraille *et al.*, 2005, Neuenhahn *et al.*, 2006, Edelson *et al.*, 2011). In support of this interpretation, filamentous bacteria stay in the blood longer than SU *Lm*, and mostly grew extracellularly within infected spleens. Interestingly, however, during *Mycobacterium tuberculosis (Mtb)* infection, a related cording phenotype is indeed essential for bacterial virulence and has been associated with the ability of *Mtb* to persist within infected hosts (Glickman *et al.*, 2000). In the case of *Lm*, cytosolic entry and growth is not only critical for successful infection of the host but also for inducing long-term protective memory (Berche *et al.*,

1987). We show that Δp60ΔNamA *Lm* are unable to enter host cells, therefore providing an explanation as to why mice immunized with this mutant of *Lm* did not develop effective T cell memory.

The second essential role of p60 and NamA autolysins highlighted by this study relates to their ability to prevent strong inflammation during cytosolic growth, a notion that was already proposed by Lenz and Portnoy (Lenz *et al.*, 2003). By immunizing with single unit (SU) Δp60ΔNamA *Lm*, we could bypass the initial block in host cell entry and investigate whether the lack of both autolysins during invasion of host cells affects the early innate immune response and T cell priming. In mice immunized with SU -but not full-length- Δp60ΔNamA *Lm*, secretion of CCL2 and CXCL1, two major chemokines involved in inflammatory $Ly6C^+$ monocyte and neutrophil mobilizations respectively (Kobayashi, 2008, Shi *et al.*, 2011), was restored to similar levels as in mice that received ΔActA *Lm*. Early recruitment of blood-derived inflammatory monocytes was shown to depend on a first wave of CCL2 secretion, the major ligand involved in $Ly6C^+$ monocytes egress from the bone marrow (Serbina *et al.*, 2006). This initial burst of CCL2 did not require cytosolic growth of *Lm* but the TLR/MyD88 signaling pathway (Jia *et al.*, 2009). This observation is consistent with our experimental set-up, in which we immunize with high numbers of poorly virulent *Lm* mutants that enter cells yet grow inefficiently. Of note, Δp60ΔNamA *Lm* were as hemolytic as WT *Lm in vitro*, likely ruling out a defect in LLO secretion and escape to the cytosol (**not shown**). Along the same lines, APC maturation, both splenic $CD11c^{hi}$ $CD8\alpha^+$ and $CD11b^+$ DCs and $Ly6C^+$ monocytes, was restored to levels close to those measured in mice immunized with ΔActA but not ΔLLO *Lm*. Thus, cytosolic escape but not growth, appears sufficient to promote robust blood phagocyte recruitment to infected tissues and strong APC maturation.

Interestingly though, we found that secretion of several inflammatory factors reflecting the triggering of innate immune sensing pathways such as type I IFN were severely impaired. This further suggested that sustained activation of such pathways requires cytosolic growth of *Lm* as previously reported (O'Riordan *et al.*, 2002). Most importantly, since we neither found reduced secretion of cyclic di-AMP by SU-Δp60ΔNamA or Δp60ΔNamA *Lm*, nor a defect of early induction of type I IFN genes in infected BMMP, the impaired production of type I IFN measured *in vivo* is most likely accounted for by inefficient intracellular growth and host tissue colonization of SU-Δp60ΔNamA *Lm*. Consistent with this interpretation, the secretion of IL-12, IFN-γ and TNF-α in mice immunized with SU-Δp60ΔNamA *Lm* was not restored to levels observed in mice immunized with ΔActA *Lm*. Indeed while upon *in vitro* cutting, access to cells of Δp60ΔNamA *Lm* could be restored to comparable efficiency than non-filamentous *Lm*, SU-Δp60ΔNamA *Lm* most likely still grew as a filament inside infected cells. Thus intracellular growth is probably most important to enhance inflammatory signals in general, which are key for optimal T cell programming (Haring *et al.*, 2006). Overall this impaired triggering of inflammation is accounted for by poor cytosolic growth of filamentous Δp60ΔNamA *Lm* which is likely associated to the lack of sustained secretion/production of immunogenic products such as cyclic dinucleotides, PGN fragments or others.

Analysis of *Lm*-induced memory $CD8^+$ T cells in mice that received the distinct immunizations revealed that while frequencies and numbers of LLO-specific effector ($CD62L^{lo}$) and memory ($CD62L^{hi}$) $CD8^+$ T cells were equivalent in all groups, their ability to produce the effector molecules CCL3 and Granzyme B (but not IFN-γ), and to express the marker of strong effector differentiation KLRG1 was diminished in mice immunized with full-length and SU Δp60ΔNamA (or control ΔSecA2) *Lm* compared to WT or ΔActA *Lm*. This phenotype correlated with their inability to control the recall infection with WT *Lm*. Both during SU Δp60ΔNamA and ΔActA *Lm* immunizations, the $CD8^+$ T cell response against LLO -which is intrinsically protective (Harty *et al.*, 1992)- and upregulation of costimulatory molecules expression on APCs were substantially restored. Inflammation, which provides critical signals during T cell priming, was strongly altered, suggesting that p60 and NamA autolysins trigger cytosolic sensing pathways involved in the secretion of key modulating cytokines. Type I IFN for instance acts as a third signal directly on T cells and sustains their proliferation and differentiation into robust effector and memory cells via anti-apoptotic effects, during various viral infections (Kolumam *et al.*, 2005, Thompson *et al.*, 2006, Kohlmeier *et al.*, 2010). Type I IFN is also a strong inducer of IL-15 *trans*-presentation by macrophages, monocytes and DCs, which modulates memory T cell homeostatic proliferation and maintenance and/or survival (Mortier *et al.*, 2009). Our data seem to be consistent with type I IFN promoting robust differentiation of effective memory cells, though recent work from the Portnoy group reported that providing increased type I IFN signals via STING/IRF3 during T cell priming by co-immunizing with ΔActA *Lm* and c-di-AMP prevented the establishment of a strong population of *Lm*-specific effector and memory $CD8^+$ T cells (Archer *et al.*, 2014), a result supporting an opposite interpretation. KLRG1 expression, however, has not been associated with type I IFN but rather with IL-12 (Joshi *et al.*, 2007). Indeed, IL-12 and subsequent IFN-γ levels in the spleens of mice that received SU Δp60ΔNamA compared to ΔActA *Lm* remained very low, which may account for the diminished expression of KLRG1 on *Lm*-specific $CD8^+$ T cells primed in these mice. While as expected (Joshi *et al.*, 2007) co-immunization with CpG, a strong inducer of IL-12, restores KLRG1 expression on these cells, most of these cells were rapidly lost from the spleen of these mice. Altogether, our results and these studies suggests that a fine combination of discrete inflammatory signals, that include type I IFN and IL-12, and likely others, are necessary to generate a highly effective and stable memory $CD8^+$ T cell population.

In summary, results from this study highlight an interesting and novel role for the p60 and NamA *Lm* autolysins in tuning an appropriate inflammatory balance required to promote long-lived functional memory $CD8^+$ T cells during *Lm* immunization. It further underlines their potential promise as novel adjuvants for optimal $CD8^+$ T cell-priming in vaccine formulations.

Experimental Procedures

Ethic Statement

Animal studies were conducted in accordance to the National Institutes of Health guidelines in compliance with assurance of the well being of laboratory animals. All protocols used in

the study have been approved by the Institutional Animal Care and Use Committee of Albert Einstein College of Medicine (protocol # 20120509). The Albert Einstein College of Medicine of Yeshiva University (Einstein) adheres to all applicable federal, state, local and institutional laws, standards, and guidelines designed to ensure humane use of animals in research, testing, and teaching. Such laws, standards, and guidelines include but are not limited to (i) the Guide for the Care and Use of Laboratory Animals, (ii) the Animal Welfare Act and (iii) PHS Policy on Humane Care and Use of Laboratory Animals.

Mice

WT BALB/c (Harlan) or C57BL/6J (Jackson) 6–8 wk-old male or female mice were used in all experiments as specified in the figure legends. In some experiments, the B6-$K^{d+/+}$ (Serbina *et al.*, 2003) transgenic line was used. All mice utilized for experiments were housed and bred in our SPF animal facility at the AECOM).

Generation of recombinant *Listeria monocytogenes*

Generation of GFP-expressing bacteria—2–5 μg of PEG-purified pNF8 (Fortineau *et al.*, 2000) was electroporated into Δp60NamA *Lm* that were prepared for electroporation according to standard procedures. Transfected-bacteria were selected onto broth heart infusion (BHI, Sigma Aldrich) plates with 10 μg/ml erythromycin and GFP-expression checked by flow cytometry (FACSCalibur). GFP^+ WT, ΔSecA2, ΔLLO *Lm* were generated previously (Muraille *et al.*, 2007). All experiments were performed with the 10403s strain of *Lm*.

Generation of Lm lacking p60 and NamA autolysins—Sequences encompassing genomic DNA flanking the gene encoding the p60 protein (*iap*) and the 5' (fragment 1) or 3' (fragment 2) end of the gene were amplified by PCR (HF Advantage 2, Clontech) to generate a deleted p60 chimeric construct that contains targeting sequences for genomic recombination and for knocking out *Lm* p60 gene. We used Fw1 5'ACGGATCCTGTTGAAGCAATGATAGTGCCG3' and Rv1 5'ATCGGCACCTGATAGCTAAGCTCATTCTGGCGCACAATACGCTA3' and, Fw2 5'TGAGCTTAGCTATCAGGTGCCGATAAATGCTGTTACCGCAATCCC3' and Rev2 5'ACGGATCCCCAAATTCAGAAGCCGTTCCA3' to amplify both fragments and clone them using the BamHI restriction site directly into the pKSV7 transfer vector. The resulting construct was verified by PCR and sequencing (AECOM sequencing facility). pKSV7 which contains the p60 targeting construct, carries a resistance to ampicillin (in *Escherichia coli*, 100μg/ml) and to chloramphenicol (Cam) (in *Lm*, 10 μg/ml) and a temperature-sensitive origin of replication (restrictive temperature of 41°C) and was transformed into Δ*murA*/ΔNamA *Lm* (Lenz *et al.*, 2002). Recombinant ΔNamA *Lm* mutated for p60 were selected through cycles of excision/recombination that include Cam and temperature restrictive growth as previously described (Rahmoun *et al.*, 2011). Deletion of the p60 gene was checked by PCR using sets of primers outside the targeted area.

Preparation of single unit (SU) ΔNamAΔp60 *Lm*

Log phase grown ΔNamAΔp60 *(*Δ*iap*Δ*murA) Lm* were pelleted and resuspended in PBS containing 5 μg/ml of purified recombinant p60 (rp60) and NamA (rNamA) and incubated

for 1 hour (37C, 100 RPM). Cells were then washed twice in PBS 1X prior to infection. For intermediate (Int-) ΔNamAΔp60 *Lm*, ΔNamAΔp60 *Lm* was grown in a 1:1 ratio of fresh BHI media and filtered (0.22 μm) BHI supernatant from OVN culture of ΔLLO *Lm*.

Cloning, expression and purification of Lm autolysins—DNA encoding for p60 and NamA devoid of the putative sequence encoding for their signal peptides were amplified by PCR (HF Advantage 2, Clontech) using the following primers: for p60, Fw 5'AGTCATATGGTAGTAGTCGAAGCTGGTGATACTC3' and Rv 5'AGTGGATCCTTATACGCGACCGAAGCC3'; and for NamA, Fw 5'AGTCATATG GACGAAACAGCGCCTG3' and 5'TCAGGATCC TCACTTAATTGTTAATTTCTGACCAAGA3' (NamA). Primers include NdeI and BamHI cloning sites and the PCR products were inserted into the IPTG-inducible expression vector pET14b (clontech) in frame (N-terminus) with MCS-encoded 6×histidine tag and a thrombin cutting site. Positive clones were screened by restriction digest and both constructs verified by sequencing. rp60 and rNamA were further produced and purified (AECOM protein core facility) by nickel affinity and size exclusion chromatography from IPTG-induced log-phase grown (OD600~0.8) BL-21 *Escherichia coli* bacterial pellets expressing either of the 2 constructs. Purified proteins were verified by mass spectrometry, aliquoted and stored in Tris buffer pH7.4 40% glycerol at −80C.

In vitro analysis of *Lm* mutants

Indicated *Lm* strains were inoculated into fresh BHI medium from log-phase frozen aliquots at a 1/10th dilution and grown 37C, 220 RPM. Colony morphology was visualized from log phase grown *Lm* plated on BHI agar plates (37C) for 12 hours. Images were taken using a Nikon light microscope. To visualize bacteria and count the number of *Lm* single unit per filament, log phase *Lm* were washed in PBS, heat fixed onto glass slides and Gram stained before imaging. For determination of *Lm* sizes by FACS, indicated GFP^+ *Lm* were grown to log phase in BHI, washed twice in PBS 1X and acquired on a FACSCalibur flow-cytometer.

Infection of Bone Marrow derived Macrophages (BMMP)

Fresh bone marrow cells were obtained from femurs of 5 weeks (wks) old WT B6 mice. Bone marrow cells were differentiated for 7–10 days into bone-marrow derived macrophages (BMMP) using L929-cell conditioned medium (30% L929 in 1640 RPMI-10% FCS Complete Medium, Gibco) in tissue culture Petri dish. Approximately 10^6 cells were seeded in 6 well plates until confluent. Cells were then infected with log phase grown *Lm* (MOI of 10) in RPMI1640 with 2.5% FCS and incubated (37C, 5% CO2) for 1 hour. Excess bacteria were removed by centrifugation, incubated for 1 hr with media supplemented with 100 μg/ml gentamicin to kill extracellular bacteria. At indicated times, MP were lysed in 1% Triton X-100 and dilutions were further plated onto BHI plates to determine *Lm* titers.

Quantitative RT-qPCR analysis

BMMP were infected as described with 5 bacteria per target cells (MOI of 5) using ΔNamAΔp60, SU-ΔNamAΔp60, ΔLLO, ΔActA and WT *Lm* and left for 6 hrs (37C, CO_2) before harvesting for RNA extraction. RNA was extracted using the RNAqueous Micro Kit (Ambion) and cDNA was synthesized with SuperScript III Reverse Transcriptase

(Invitrogen). Quantitative RT-PCR was performed with an Applied Biosystem Prism 7300 fast real time PCR system using Power SYBR green PCR Master Mix (Life Technologies). Primer sequences for *Ifn*α and *Ifn*β genes were chosen according to previous studies (Kim *et al.*, 2012). Briefly, "Universal" primers were designed to target multiple *Ifn*α variants (GTGAGGAAATACTTCCACAG, GGCTCTCCAGACTTCTGCTC). The following primers were chosen for Actin (GGCTGTATTCCCCTCCATCG, CCAGTTGGTAACAATGCCATGT) and *Ifn*β (CAGCTCCAAGAAAGGACGAAC, GGCAGTGTAACTCTTCTGCAT). The cycling threshold (Ct) of gene transcripts was determined by RT-qPCR and normalized to the Ct of beta-actin for calculation of the ΔCt values. The relative expression of genes for each sample was determined by calculation of the $2^{-\Delta\Delta Ct}$ value.

Mice infections and other treatments

All WT *Lm* were prepared from clones grown to log phase from organs of infected mice and kept at −80°C. For *Lm* infections, bacteria were grown to a logarithmic phase (OD600~0.05–0.15) in BHI medium, diluted in PBS to infecting concentration (an OD600 of 0.1 corresponds to ~2×10^8 *Lm*/ml for WT *Lm*) and injected i.v. either in the retro-orbital or tail veins. For filamentous mutants, i.e., Δp60ΔNamA and ΔSecA2 *Lm*, we have established by comparative plating of exponentially growing Δp60ΔNamA with or without *in vitro* cutting with recombinant p60 and NamA proteins, that an OD600 of 0.1 corresponded to ~1.12×10^8 *Lm*/ml (**not shown**).

Determining Lm titers in organs and blood—To determine bacterial titers, organs were harvested under sterile conditions and dissociated on sterile metal meshes in 0.1% triton X-100 in water. Successive dilutions were plated onto BHI agar plates to determine the total bacterial CFU per organ. For blood, mice were bled retro-orbitally (200 µl), which was lysed vol/vol with in 0.1% triton X-100/water, diluted and plated on BHI Petri dishes.

Other treatments—For gentamicin, mice were injected i.p. 2 mg in 500 µl PBS. For CpG, 50µg of CpG ODN 1826 (Invivogen) were injected i.v. 1 hr post immunization with ΔNamAΔp60 *Lm*.

UPLC Mass Spectrometry (MS) analysis of secreted c-di-AMP

Preparation of samples for MS analysis—WT, ΔActA, Δp60ΔNamA on 10403s background or WT L028 *Lm* were inoculated in BHI from −80C frozen stocks and grown OVN (37C, 180RPM). The next day, stationary phase *Lm* were transferred to fresh BHI medium (1/10) and grown to OD600~0.5, washed once into Improved Minimal Media (IMM) (Phan-Thanh *et al.*, 1997) before growth in IMM for 19 hrs (37°C, 180RPM). Identical numbers of *Lm* from cultures were corrected based on OD600 measurements, centrifuged, supernatants filtered (0.22µm), and 1 ml was further dried to 1200 µl (speedvac). Protein precipitation was performed by adding 400 µl of methanol and 400 µl of acetonitrile per sample, insoluble material was pelleted by centrifugation (13,000 RPM, 1'), and supernatant was filtered again through a 0.22µm spin column filter.

UPLC-MS analysis—Culture supernatants were analyzed by UPLC-MS to quantitate c-di-AMP using previously reported method (Paglia *et al.*, 2012). A Waters Acquity UPLC system coupled to a Waters Synapt G2 quadrupole-time of flight hybrid mass spectrometer was used to separate and detect metabolites. A Waters Acuity amide column 1.7μm (2.1 × 150mm) was used to separate metabolites in HILIC mode, eluted at 0.5mL/min with 100% acetonitrile, 0.1% formic acid as mobile phase A and 100% water, 0.1% formic acid as mobile phase B. The gradient began with 1% B until 1 min, ramped to 35% B by 14 min, then 60% B by 17 min, held at 60% B for 1 minute, then ramped to 1% B by 19 min and held at 1% B to the end of run at 20 min. The mass spectrometer was operated in positive ion resolution mode with 2kV capillary voltage and 17V cone voltage. Cone gas flow was 20L/hr; desolvation gas flow was 800L/hr. Source temperature was 120°C and desolvation gas temperature was 500°C. Using a scan time of 0.5s, mass spectra were acquired in MS^e centroid mode from 50 – 1200 m/z. The lock mass compound leucine enkephalin at 2ng/μL was detected at 556.2771 m/z. An authentic standard of c-di-AMP (Invivogen) was used to determine retention time and high-energy fragmentation pattern under our conditions. Extracted ion chromatograms for 659.11 ± 0.02 m/z and the 330.06 m/z fragment ion peaks corresponding to this retention time (13.9 min) with the same high-energy fragmentation patterns were integrated to determine relative quantities of c-di-AMP secreted by each strain.

Cell preparation for flow-cytometry analysis

For blood, approximately 200 μl was collected from mice via retro-orbital bleeding and lysed for 5 min in 0.83% NH_4Cl v/v with culture media. For spleens, they were harvested and dissociated on nylon meshes and incubated (37C, 30') in HBSS (Gibco) medium containing 4000 U/ml of collagenase IV (Roche) and 0.1 mg/ml of DNase (Sigma). Red blood cells were then lysed for 5 min.

Flow cytometry analysis

Cell suspensions prepared as above were recovered in FACS buffer (PBS 1% FCS, 2mM EDTA, 0.02% sodium azide). Briefly, $3–5\times10^6$ spleen cells or 10^5 blood cells were incubated with 2.4G2 for 15 min on ice and further stained with specified antibodies cocktail using directly coupled fluorescent mAbs combinations in 100 μl PBS 0.5% BSA 0.02% NaN_3 (FACS buffer). For intracellular staining (IC), cells were incubated for 3–4 hrs at 37°C, 5% CO_2 in RPMI1640 (Invitrogen) 5% FCS, Golgi Plug (BD), fixed in IC fixation buffer (eBioscience) for 15 min at 4°C, and permeabilized for 30 min in 1X Perm/Wash buffer (BD or eBioscience) containing the intracellular mAbs. Stained samples were further collected on either FACSCalibur, LSR-II, or Aria III flow cytometers (Becton Dickinson, BD). The following mAbs were used and purchased either from BD Pharmingen or eBioscience: anti-CD8α (53–6.7)-fluorescein isothiocyanate (FITC), phycoerythrin (PE), peridinin chlorophyl protein (PcP) or allophycocyanin (APC), anti-CD3ε-FITC (145-2C11), anti-CD62L-A700 (MEL-14), anti-CD11c-Pe-Cy7 (N418), anti-CD11b-eFluor 450 or PcP-Cy5.5 (M1/70), anti-Ly-6C-FITC (AL-21), anti-CD45.2-A700 (104), anti-MHC Class II-A700 (M5/114.12.2), anti-CD80-PE (1615A1), anti-CD86-A700 (GL1), anti-CD40-A700 (1C10), anti-ScaI-A700 (D7), anti-IL-15Rα-PE (DNT15Rα), anti-KLRG1-PE-Cy7 (MAFA 2F1), anti-IFNγ-APC or A700 (XMG1.2).

Anti-Granzyme B-APC (mouse and human) and anti-CCL3 (polyclonal goat) were purchased from Invitrogen and R&D systems respectively. H2-K^d/$LLO_{91–99}$ tetramers coupled to PE were obtained from the NIH tetramer core facility.

Measure of splenic cytokines and chemokines contents

Spleens from immunized mice were harvested, snap-frozen and stored at −80C until further processing. Spleens were then thawed in 150 μl of processing buffer (150mM NaCl, 40mM Tris pH 7.4) containing a cocktail of protease inhibitors (Promega), homogenized with a douncer and froze/thawed once before centrifugation to obtain cleared supernatants to aliquot and store at −80C. Dosing of indicated cytokines/chemokines in cleared supernatants was performed using flow-cytomix (ebioscience) on an Aria III flow cytometer and according to the manufacturer protocol. IL-12 was measured using an IL-12p70 specific ELISA (ebioscience).

Statistics

Statistical significance was calculated using an unpaired Student t test with GraphPad Prism software and two-tailed p values are given as: (*) $p<0.1$; (**) $p<0.01$; and (***) $p<0.001$; (ns) $p>0.1$. All p values of 0.05 or less were considered significant and are referred to as such in the text.

Supplementary Material

Refer to Web version on PubMed Central for supplementary material.

Acknowledgments

H2-K^d/$LLO_{91–99}$ tetramers were obtained through the NIH Tetramer Facility. This work was supported by institutional funds of the Albert Einstein College of Medicine of Yeshiva University (GL), the National Institute of Health (Grants R21AI095835 and R01AI103338). Core resources that facilitated flow cytometry were supported by the Einstein Cancer Center (NCI cancer center support grant 2P30CA013330).

References

Archer KA, Durack J, Portnoy DA. STING-dependent type I IFN production inhibits cell-mediated immunity to Listeria monocytogenes. PLoS Pathog. 2014; 10:e1003861. [PubMed: 24391507]

Berche P, Gaillard JL, Sansonetti PJ. Intracellular growth of Listeria monocytogenes as a prerequisite for in vivo induction of T cell-mediated immunity. J Immunol. 1987; 138:2266–2271. [PubMed: 3104455]

Beuneu H, Deguine J, Bouvier I, Di Santo JP, Albert ML, Bousso P. A dual role for type I IFNs during polyinosinic-polycytidylic acid-induced NK cell activation. J Immunol. 2011; 187:2084–2088. [PubMed: 21810605]

Campisi L, Soudja SM, Cazareth J, Bassand D, Lazzari A, Brau F, et al. Splenic CD8alpha(+) dendritic cells undergo rapid programming by cytosolic bacteria and inflammation to induce protective CD8(+) T-cell memory. Eur J Immunol. 2011; 41:1594–1605. [PubMed: 21469106]

Edelson BT, Bradstreet TR, Hildner K, Carrero JA, Frederick KE, Kc W, et al. CD8alpha(+) Dendritic Cells Are an Obligate Cellular Entry Point for Productive Infection by Listeria monocytogenes. Immunity. 2011; 35:236–248. [PubMed: 21867927]

Fortineau N, Trieu-Cuot P, Gaillot O, Pellegrini E, Berche P, Gaillard JL. Optimization of green fluorescent protein expression vectors for in vitro and in vivo detection of Listeria monocytogenes. Res Microbiol. 2000; 151:353–360. [PubMed: 10919515]

Glickman MS, Cox JS, Jacobs WR Jr. A novel mycolic acid cyclopropane synthetase is required for cording, persistence, and virulence of Mycobacterium tuberculosis. Mol Cell. 2000; 5:717–727. [PubMed: 10882107]

Haring JS, Badovinac VP, Harty JT. Inflaming the CD8+ T cell response. Immunity. 2006; 25:19–29. [PubMed: 16860754]

Harty JT, Badovinac VP. Shaping and reshaping CD8+ T-cell memory. Nat Rev Immunol. 2008; 8:107–119. [PubMed: 18219309]

Harty JT, Bevan MJ. CD8+ T cells specific for a single nonamer epitope of Listeria monocytogenes are protective in vivo. J Exp Med. 1992; 175:1531–1538. [PubMed: 1375265]

Heath WR, Belz GT, Behrens GM, Smith CM, Forehan SP, Parish IA, et al. Cross-presentation, dendritic cell subsets, and the generation of immunity to cellular antigens. Immunol Rev. 2004; 199:9–26. [PubMed: 15233723]

Hildner K, Edelson BT, Purtha WE, Diamond M, Matsushita H, Kohyama M, et al. Batf3 deficiency reveals a critical role for CD8alpha+ dendritic cells in cytotoxic T cell immunity. Science. 2008; 322:1097–1100. [PubMed: 19008445]

Iwasaki A, Medzhitov R. Toll-like receptor control of the adaptive immune responses. Nat Immunol. 2004; 5:987–995. [PubMed: 15454922]

Iwasaki A, Medzhitov R. Regulation of adaptive immunity by the innate immune system. Science. 2010; 327:291–295. [PubMed: 20075244]

Jia T, Leiner I, Dorothee G, Brandl K, Pamer EG. MyD88 and Type I interferon receptor-mediated chemokine induction and monocyte recruitment during Listeria monocytogenes infection. J Immunol. 2009; 183:1271–1278. [PubMed: 19553532]

Joshi NS, Cui W, Chandele A, Lee HK, Urso DR, Hagman J, et al. Inflammation directs memory precursor and short-lived effector CD8(+) T cell fates via the graded expression of T-bet transcription factor. Immunity. 2007; 27:281–295. [PubMed: 17723218]

Kim CC, Nelson CS, Wilson EB, Hou B, DeFranco AL, DeRisi JL. Splenic red pulp macrophages produce type I interferons as early sentinels of malaria infection but are dispensable for control. PLoS One. 2012; 7:e48126. [PubMed: 23144737]

Kobayashi Y. The role of chemokines in neutrophil biology. Front Biosci. 2008; 13:2400–2407. [PubMed: 17981721]

Kohlmeier JE, Cookenham T, Roberts AD, Miller SC, Woodland DL. Type I interferons regulate cytolytic activity of memory CD8(+) T cells in the lung airways during respiratory virus challenge. Immunity. 2010; 33:96–105. [PubMed: 20637658]

Kolumam GA, Thomas S, Thompson LJ, Sprent J, Murali-Krishna K. Type I interferons act directly on CD8 T cells to allow clonal expansion and memory formation in response to viral infection. J Exp Med. 2005; 202:637–650. [PubMed: 16129706]

Lenz LL, Mohammadi S, Geissler A, Portnoy DA. SecA2-dependent secretion of autolytic enzymes promotes Listeria monocytogenes pathogenesis. Proc Natl Acad Sci U S A. 2003; 100:12432–12437. [PubMed: 14527997]

Lenz LL, Portnoy DA. Identification of a second Listeria secA gene associated with protein secretion and the rough phenotype. Mol Microbiol. 2002; 45:1043–1056. [PubMed: 12180923]

Machata S, Hain T, Rohde M, Chakraborty T. Simultaneous deficiency of both MurA and p60 proteins generates a rough phenotype in Listeria monocytogenes. J Bacteriol. 2005; 187:8385–8394. [PubMed: 16321943]

Mortier E, Advincula R, Kim L, Chmura S, Barrera J, Reizis B, et al. Macrophage- and dendritic-cell-derived interleukin-15 receptor alpha supports homeostasis of distinct CD8+ T cell subsets. Immunity. 2009; 31:811–822. [PubMed: 19913445]

Moseman EA, McGavern DB. The great balancing act: regulation and fate of antiviral T-cell interactions. Immunol Rev. 2013; 255:110–124. [PubMed: 23947351]

Muraille E, Giannino R, Guirnalda P, Leiner I, Jung S, Pamer EG, Lauvau G. Distinct in vivo dendritic cell activation by live versus killed Listeria monocytogenes. Eur J Immunol. 2005; 35:1463–1471. [PubMed: 15816001]

Muraille E, Narni-Mancinelli E, Gounon P, Bassand D, Glaichenhaus N, Lenz LL, Lauvau G. Cytosolic expression of SecA2 is a prerequisite for long-term protective immunity. Cell Microbiol. 2007; 9:1445–1454. [PubMed: 17244189]

Narni-Mancinelli E, Campisi L, Bassand D, Cazareth J, Gounon P, Glaichenhaus N, Lauvau G. Memory CD8+ T cells mediate antibacterial immunity via CCL3 activation of TNF/ROI+ phagocytes. J Exp Med. 2007; 204:2075–2087. [PubMed: 17698589]

Neuenhahn M, Kerksiek KM, Nauerth M, Suhre MH, Schiemann M, Gebhardt FE, et al. CD8alpha+ dendritic cells are required for efficient entry of Listeria monocytogenes into the spleen. Immunity. 2006; 25:619–630. [PubMed: 17027298]

O'Riordan M, Yi CH, Gonzales R, Lee KD, Portnoy DA. Innate recognition of bacteria by a macrophage cytosolic surveillance pathway. Proc Natl Acad Sci U S A. 2002; 99:13861–13866. [PubMed: 12359878]

Paglia G, Hrafnsdottir S, Magnusdottir M, Fleming RM, Thorlacius S, Palsson BO, Thiele I. Monitoring metabolites consumption and secretion in cultured cells using ultra-performance liquid chromatography quadrupole-time of flight mass spectrometry (UPLC-Q-ToF-MS). Anal Bioanal Chem. 2012; 402:1183–1198. [PubMed: 22159369]

Pamer EG. Immune responses to Listeria monocytogenes. Nat Rev Immunol. 2004; 4:812–823. [PubMed: 15459672]

Phan-Thanh L, Gormon T. A chemically defined minimal medium for the optimal culture of Listeria. Int J Food Microbiol. 1997; 35:91–95. [PubMed: 9081230]

Rahmoun M, Gros M, Campisi L, Bassand D, Lazzari A, Massiera C, et al. Priming of protective anti-Listeria monocytogenes memory CD8+ T cells requires a functional SecA2 secretion system. Infect Immun. 2011; 79:2396–2403. [PubMed: 21402759]

Reis e Sousa C. Dendritic cells in a mature age. Nat Rev Immunol. 2006; 6:476–483. [PubMed: 16691244]

Sallusto F, Lanzavecchia A, Araki K, Ahmed R. From vaccines to memory and back. Immunity. 2010; 33:451–463. [PubMed: 21029957]

Schwartz KT, Carleton JD, Quillin SJ, Rollins SD, Portnoy DA, Leber JH. Hyperinduction of host beta interferon by a Listeria monocytogenes strain naturally overexpressing the multidrug efflux pump MdrT. Infect Immun. 2012; 80:1537–1545. [PubMed: 22290148]

Serbina NV, Pamer EG. Monocyte emigration from bone marrow during bacterial infection requires signals mediated by chemokine receptor CCR2. Nat Immunol. 2006; 7:311–317. [PubMed: 16462739]

Serbina NV, Salazar-Mather TP, Biron CA, Kuziel WA, Pamer EG. TNF/iNOS-producing dendritic cells mediate innate immune defense against bacterial infection. Immunity. 2003; 19:59–70. [PubMed: 12871639]

Shen H, Slifka MK, Matloubian M, Jensen ER, Ahmed R, Miller JF. Recombinant Listeria monocytogenes as a live vaccine vehicle for the induction of protective anti-viral cell-mediated immunity. Proc Natl Acad Sci U S A. 1995; 92:3987–3991. [PubMed: 7732018]

Shi C, Pamer EG. Monocyte recruitment during infection and inflammation. Nat Rev Immunol. 2011; 11:762–774. [PubMed: 21984070]

Soudja SM, Ruiz AL, Marie JC, Lauvau G. Inflammatory Monocytes Activate Memory CD8(+) T and Innate NK Lymphocytes Independent of Cognate Antigen during Microbial Pathogen Invasion. Immunity. 2012; 37:549–562. [PubMed: 22940097]

Thompson LJ, Kolumam GA, Thomas S, Murali-Krishna K. Innate inflammatory signals induced by various pathogens differentially dictate the IFN-I dependence of CD8 T cells for clonal expansion and memory formation. J Immunol. 2006; 177:1746–1754. [PubMed: 16849484]

Tough DF. Modulation of T-cell function by type I interferon. Immunol Cell Biol. 2012; 90:492–497. [PubMed: 22391814]

Woodward JJ, Iavarone AT, Portnoy DA. c-di-AMP secreted by intracellular Listeria monocytogenes activates a host type I interferon response. Science. 2010; 328:1703–1705. [PubMed: 20508090]

Wuenscher MD, Kohler S, Bubert A, Gerike U, Goebel W. The iap gene of Listeria monocytogenes is essential for cell viability, and its gene product, p60, has bacteriolytic activity. J Bacteriol. 1993; 175:3491–3501. [PubMed: 8099071]

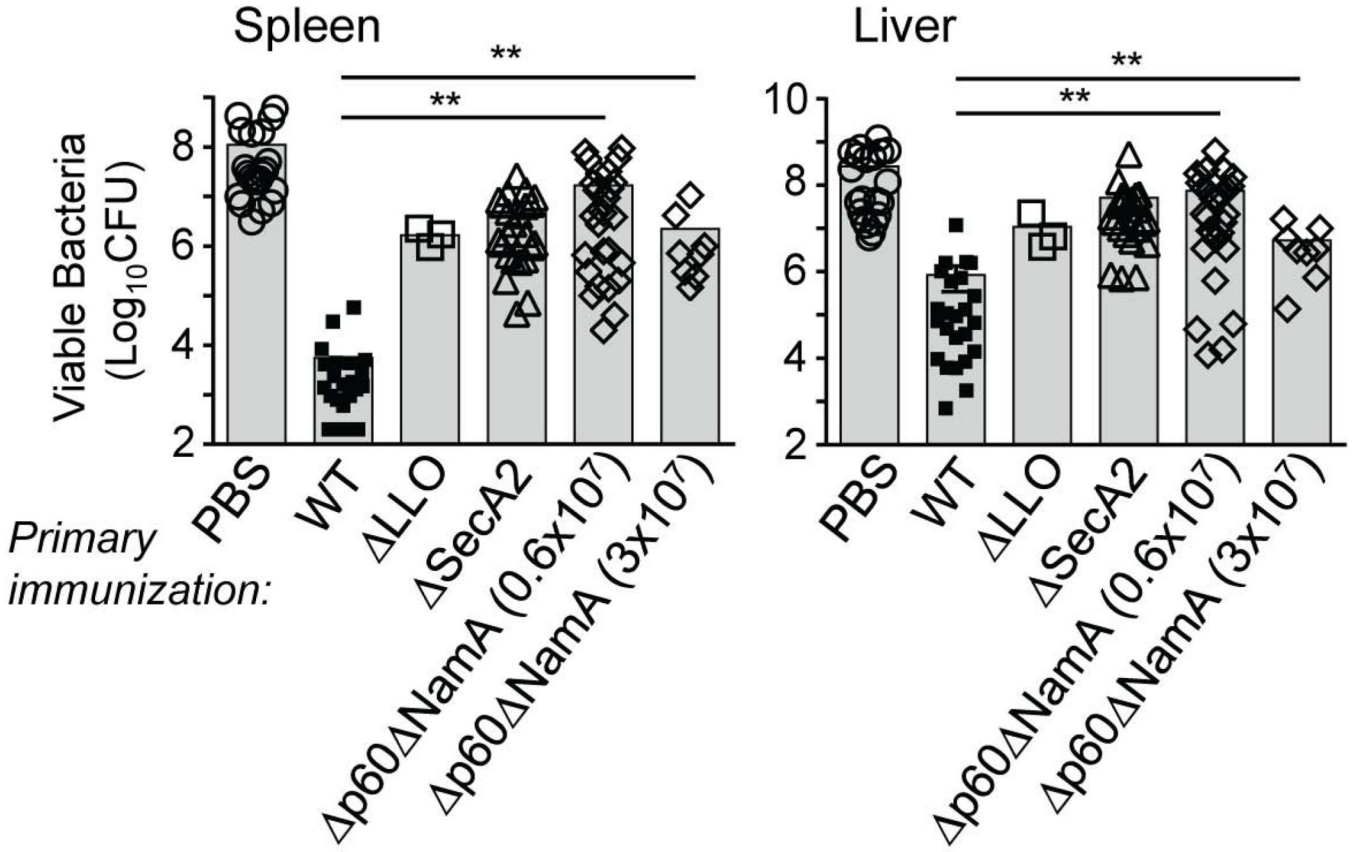

Figure 1. Mice immunized with *Lm* lacking p60 and NamA autolysins fail to mount protective memory responses

WT BALB/c mice were primary immunized i.v. with $0.1\times LD_{50}$ WT (5,000), ΔLLO (5×10^8), ΔSecA2 (0.6×10^6) and two distinct doses of Δp60ΔNamA (0.6×0^7, 3×10^7) *Lm*, or injected with PBS (unimmunized control). Five weeks later, mice were challenged with $10\times LD_{50}$ WT *Lm* (3×10^5), and spleen and liver were harvested 48 hrs later, lysed and plated to determine the number of viable bacterial CFUs. Each symbol represents one individual mouse and shaded bars the average (Mean value). Data result from the pool of 2–6 independent replicate experiments and p-values are indicated ((*) $p<0.1$; (**) $p<0.01$; (***) $p<0.001$; (****) $p<0.001$; (ns) $p>0.1$).

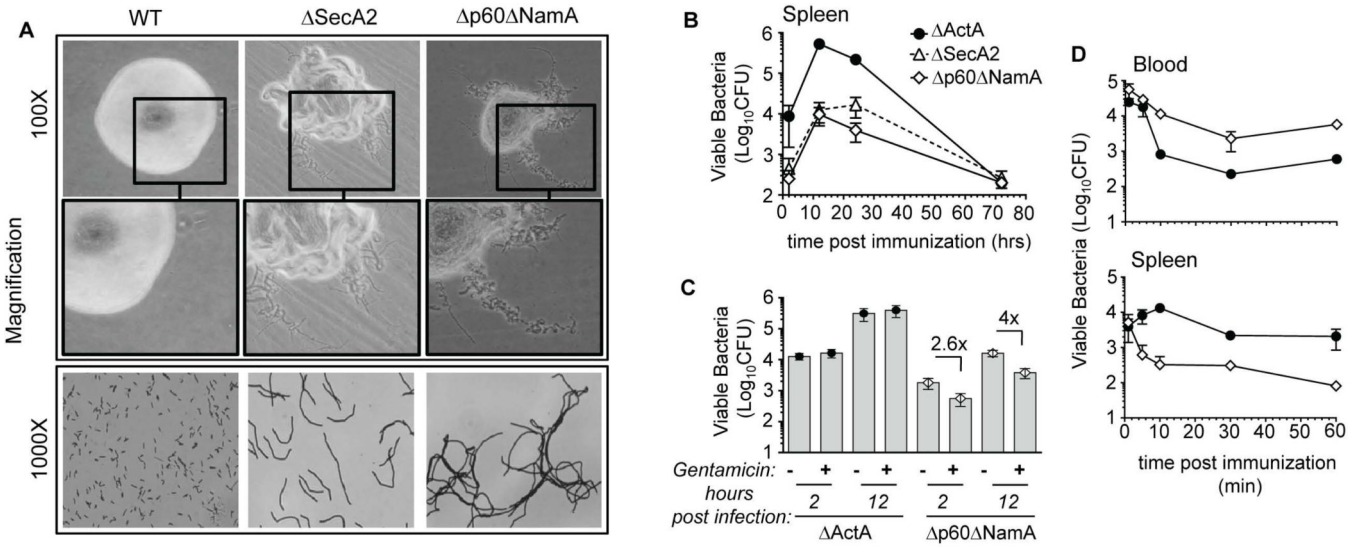

Figure 2. *Lm* lacking p60 and NamA autolysins exhibit a filamentous phenotype promoting extracellular growth within infected spleens

(**A**) Morphology of *Lm* colonies grown OVN onto BHI Petri dishes, and corresponding gram staining of bacteria. (**B–D**) WT C57BL/6 (B6) mice were infected with $0.1\times LD_{50}$ ΔActA (10^6), ΔSecA2 (0.6×10^6) and Δp60ΔNamA (0.6×10^7) *Lm*; spleen harvested at the indicated times, lysed and plated. In (C), mice received gentamycin i.p. (2 mg) 1 hr after *Lm* infection. In (D) immunized mice were bled (200μl/mouse), spleens harvested at indicated times, and *Lm* CFU determined by plating both cell suspensions after lysis. Data plots and histogram bars average mean values+/−SEM (B-D).

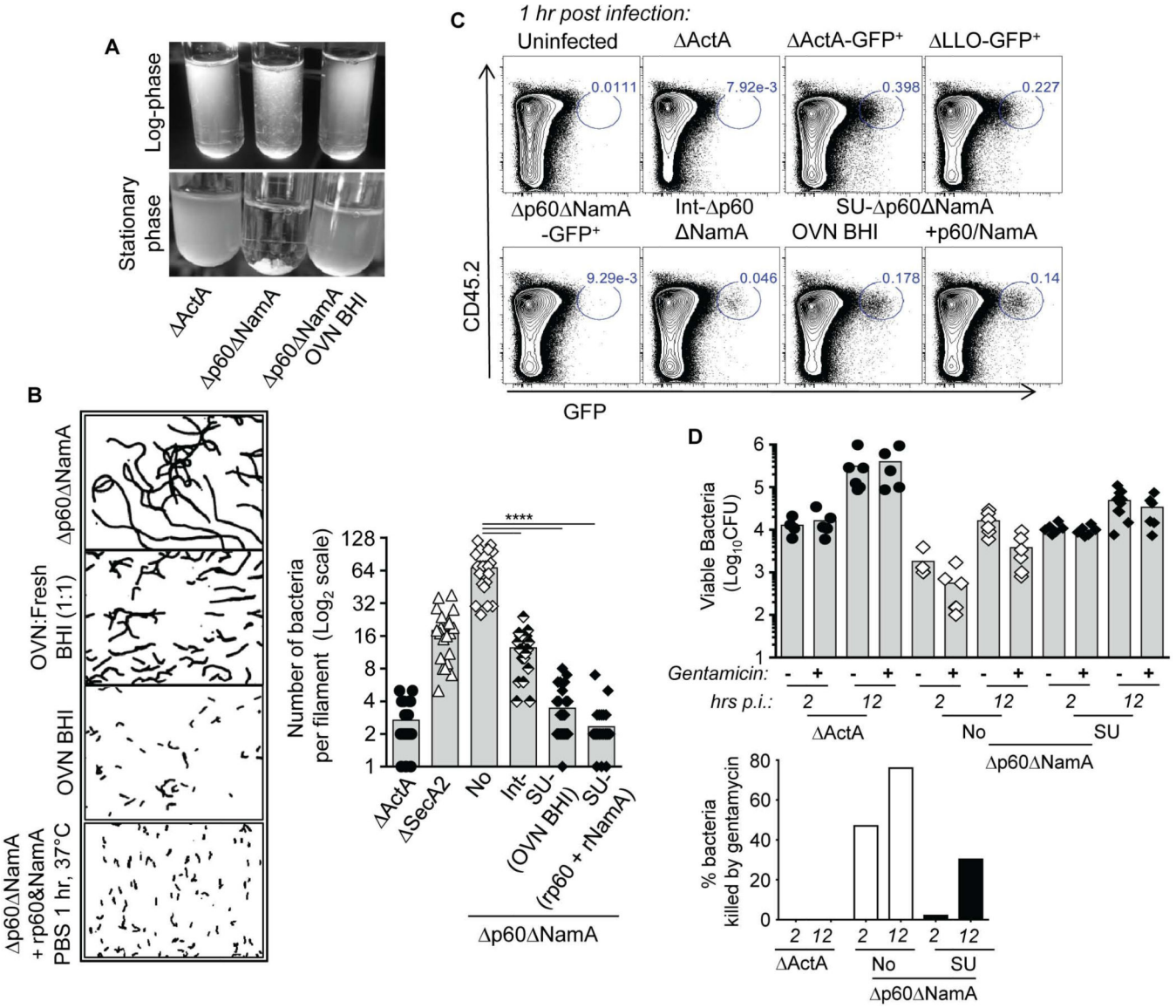

Figure 3. Filamentation prevents cell invasion and efficient host spleen colonization

(**A**) Pictures of log or stationary phase cultures of indicated *Lm* mutants grown in fresh BHI or in filtered BHI from OVN grown ΔLLO *Lm* containing secreted p60 and NamA. (**B**) Gram staining of log-phase Δp60ΔNamA *Lm* grown in indicated conditions. (**C**) WT B6 mice were inoculated with 0.6–1×10^8 of indicated GFP^+ *Lm* mutants and 1 hr later spleens were harvested, cells stained with cell-surface CD45.2 and analyzed by FACS to determine the frequencies of GFP^+ cells (blue numbers) amongst live spleen cells, e.g., cells that contain viable *Lm*. In (**D**), mice received gentamycin 1 hr post immunization and spleens were harvested and plated at indicated times to determine *Lm* titers (upper graph). The lower graph represents the same data as a relative proportion (%) of *Lm* killed by gentamicin, e.g., extracellular bacteria. All experiments show representative data of 1 of 2 independent replicate experiments; in (D) the pool of the 2 experiments is shown with each symbol representing 1 mouse. Histogram bars average mean values (B, D).

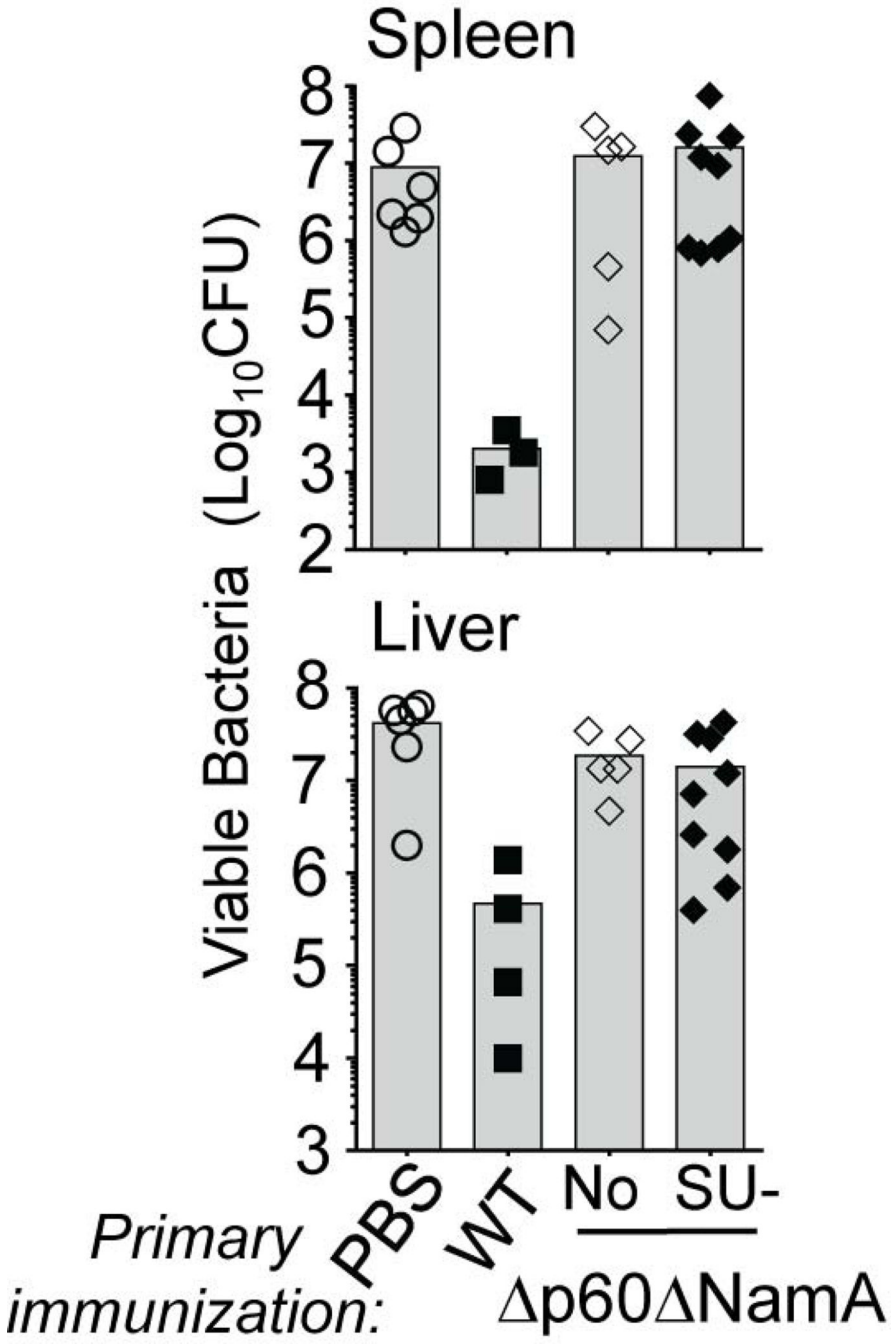

Figure 4. Rescuing cell invasion by filamentous Δp60ΔNamA *Lm* is not sufficient for protective T cell memory development

Titers of viable WT *Lm* CFU in the spleen and liver of mice immunized with $0.1\times LD_{50}$ of indicated *Lm*, and challenged 5 weeks later with 3×10^5 WT *Lm* for 48 hrs. All experiments show representative data of 1 experiment; each symbol represents 1 mouse and histogram bars average mean values.

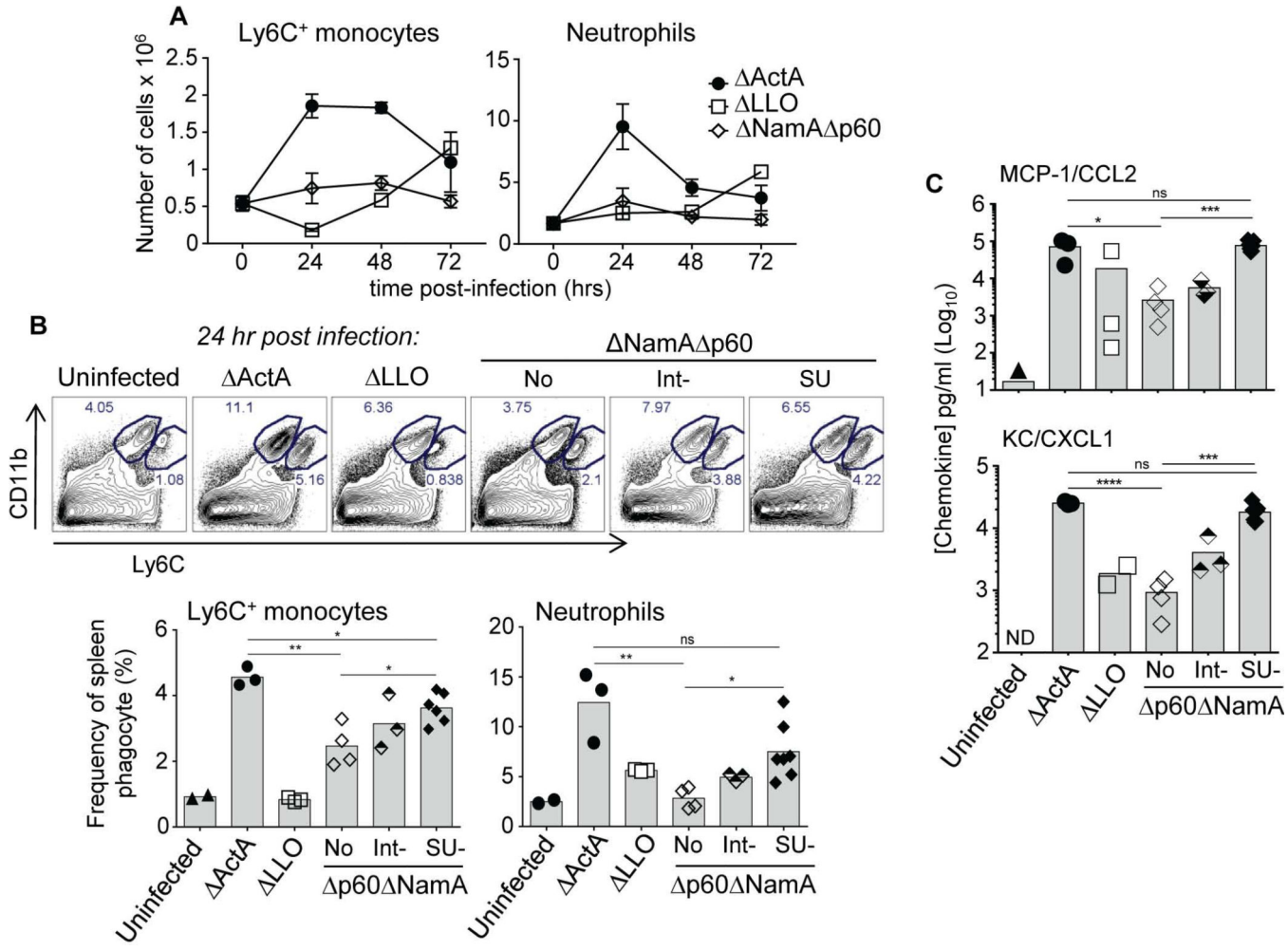

Figure 5. Cytosolic expression of p60 and NamA autolysins by *Lm* promotes efficient recruitment of blood phagocytes

(**A**) Kinetics of Ly6C$^+$ monocyte and neutrophil recruitments to the spleens of WT B6 mice immunized with 0.1×LD_{50} of indicated mutants of *Lm* (as before). (**B**) Comparative analysis of peak recruitments (24 hrs) of blood phagocytes upon the distinct immunizations. Representative dot plots are shown and bar graphs average the frequencies of each subset in 1 of 2 representative experiments. (**C**) CCL2 and CXCL1/KC chemokine levels measured directly in spleen lysates from mice immunized with indicated mutants of *Lm*. P-values are indicated. Data plots and histogram bars average mean values +/−SEM and each symbol representing one individual mouse.

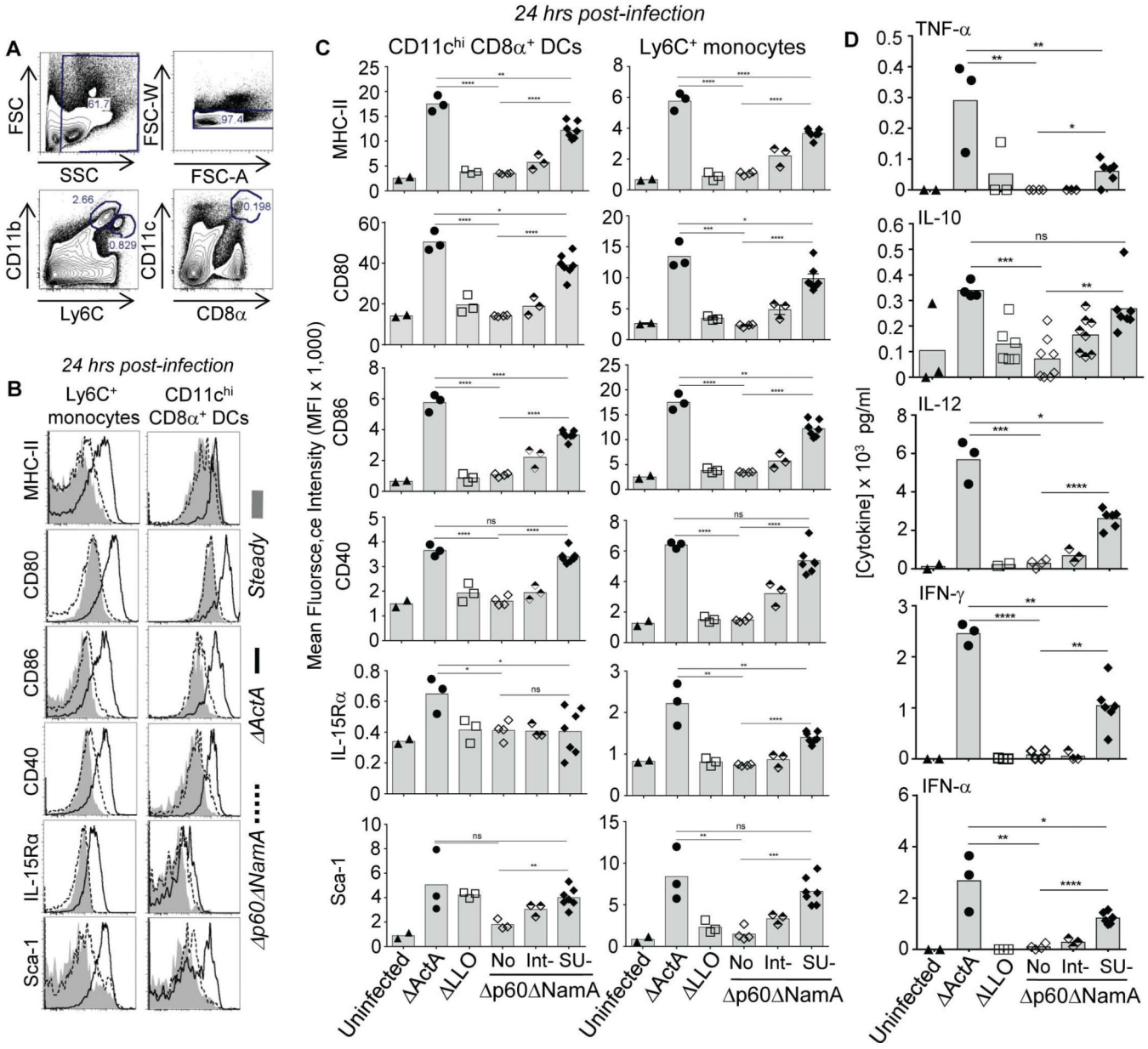

Figure 6. p60 and NamA autolysins secreted by cytosolic *Lm* promotes robust activation of antigen presenting cells but only limited inflammation

(**A**) Gating strategy of spleen Ly6C$^+$ monocytes and CD8α$^+$ DCs. (**B, C**) WT B6 mice were immunized with various mutants of *Lm*, or left unimmunized, and 24 hrs later spleens were harvested and cell suspensions stained for expression of indicated cell surface markers. (**B**) Overlays of representative FACS histograms of resting versus activated monocytes and DCs in mice that received ΔActA and Δp60ΔNamA *Lm*. (**C**) The average expression levels (MFI) of indicated cell-surface activation markers on monocytes and DCs in mice immunized with the whole panel of *Lm* mutants. (**D**) Cytokine and chemokine levels measured directly in spleen lysates from mice immunized with specified mutants of *Lm*. All experiments represent the pool of 2 replicate experiments and p-values are indicated. Histogram bars average mean values (C, D) with each symbol representing an individual mouse.

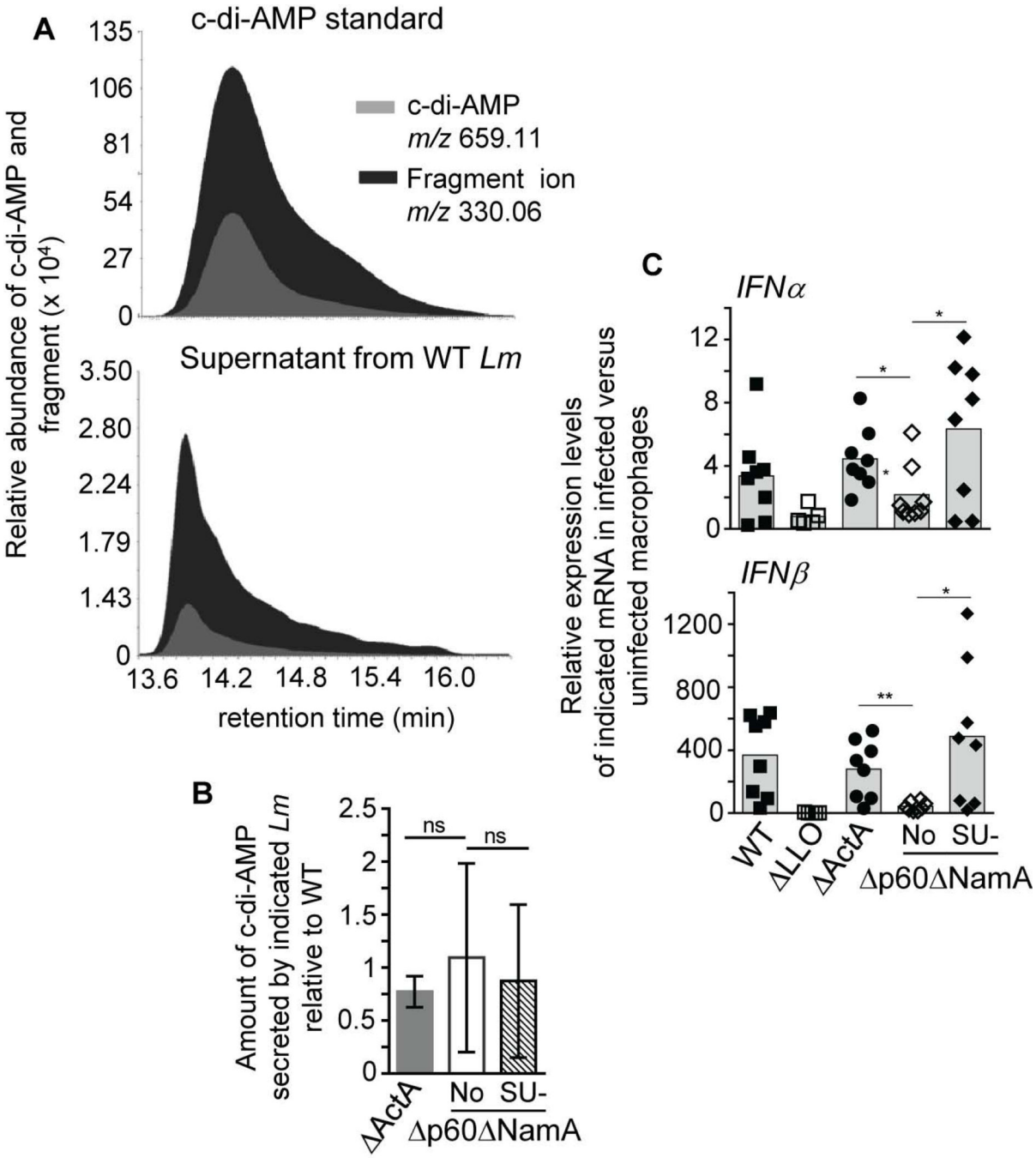

Figure 7. Lack of p60 and NamA autolysins neither impairs secretion of cyclic di-AMP, nor early induction of type I IFN genes

(A) Extracted ion chromatograms for c-di-AMP (m/z 659.11) and its in-source 330.06 m/z fragment ion on commercial c-di-AMP (upper panel) and WT *Lm* culture supernatant (lower panel). (**B**) Amount of secreted c-di-AMP 330.06 m/z fragment ion in the supernatant of log-phase grown ΔActA, Δp60ΔNamA and SU Δp60ΔNamA *Lm* relative to WT in 4 independent replicate experiments. (**C**) Relative IFNα and IFNβ mRNA expression levels in bone-marrow derived macrophages (WT B6) infected for 6 hrs with indicated mutants or

WT *Lm* (MOI of 5). Histogram bars average mean values with either mean+/− SEM (B) or each symbol representing an individual macrophage tissue culture well replicate (C).

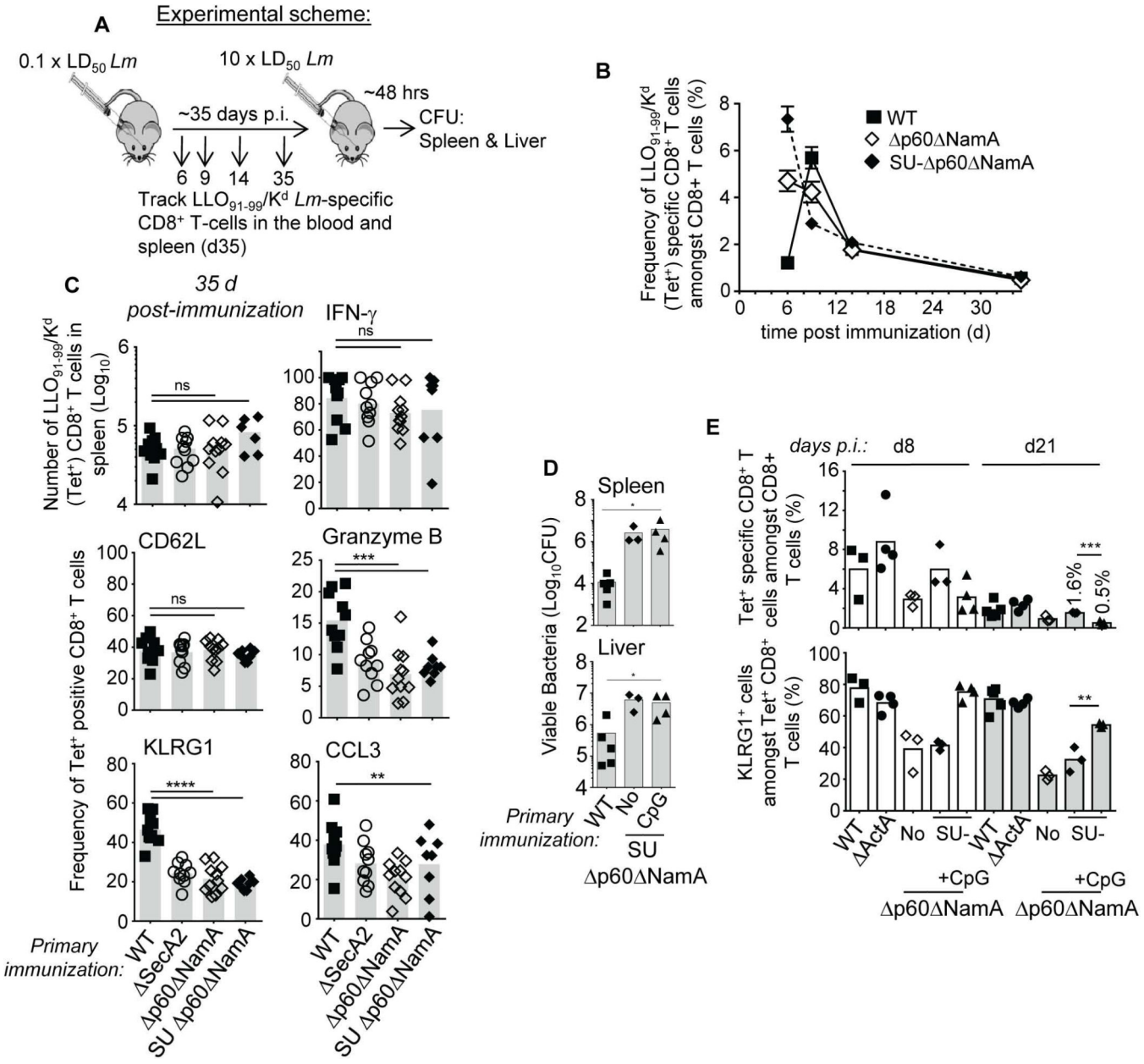

Figure 8. *Lm* autolysins provide essential inflammatory signals that promote long-term protective memory CD8$^+$ T cells

(**A**) Experimental design for (B-E). (**B**) Kinetics of *Lm*-specific $LLO_{91–99}/K^{d+}$ (tet^+) $CD8^+$ T cells in the blood of WT BALB/C mice immunized with indicated *Lm*. (**C**) Phenotypic and functional characterization of LLO-specific tet^+ splenic memory $CD8^+$ T cells 35 d post immunization with $0.1\times LD_{50}$ WT, ΔSecA2, Δp60ΔNamA and SU Δp60ΔNamA *Lm*. In (B, C), blood or spleens were harvested and cells either stained for cell-surface CD8, tet, CD62L, KLRG1 or restimulated ex vivo for 4–6 hrs with the $LLO_{91–99}$ epitope and stained for intracellular granzyme B, IFN-γ and CCL3 and surface CD8. (**D**) Titers of viable WT *Lm* CFU in the spleen and liver of mice immunized with indicated *Lm* with or without CpG nucleotides, and challenged with WT *Lm* for 48 hrs. (**E**) Frequencies of LLO-tet^+ $CD8^+$ T

cells and expression of KLRG1 in the blood 8 and 21 d after immunization with indicated *Lm*. Data shown are the pool of 2–4 replicate experiments, each symbol featuring an individual mouse and p-values are indicated. Data plots (B) or histogram bars (C-E) average mean values+/− SEM or mean with each symbol representing an individual mouse.